

Triplet superconductivity in oxide ferromagnetic interlayer of mesa-structure

G A Ovsyannikov^{1,2,4}, K Y Constantinian¹, A E Sheerman¹, A V Shadrin^{1,2},
Yu V Kislinski¹, Yu N Khaydukov³, L Mustafa³, A Kalabukhov² and D Winkler²

¹Kotel'nikov Institute of Radio Engineering and Electronics, Russian Academy of Sciences, Moscow, Russia

²Chalmers University of Technology, Department of Microtechnology and Nanoscience, Gothenburg, Sweden

³Max-Planck Institute for Solid State Research, Stuttgart, Germany

E-mail: gena@hitech.cplire.ru

Abstract. We present experimental data on Nb-Au/La_{0.7}Sr_{0.3}MnO₃/SrRuO₃/YBa₂Cu₃O_{7- δ} mesa-structure with in plane linear size 10÷50 μ m. The mesa-structures were patterned from the epitaxial heterostructures fabricated by pulsed laser ablation and magnetron sputtering. Superconducting critical current was observed for mesa-structures with the interlayer thicknesses up to 50 nm. In the mesa-structures with just one, either La_{0.7}Sr_{0.3}MnO₃ or SrRuO₃ interlayer with a thickness larger than 10 nm no superconducting current was observed. The registered superconducting current for the mesa-structures with a thinner interlayer is attributed to pinholes. Obtained results are discussed in terms of superconducting long-range triplet generation at interfaces of superconductor and a composite ferromagnet consisting of ferromagnetic materials with non-collinear magnetization.

1. Introduction

Two theoretical groups had shown that in a ferromagnet with the spatial inhomogeneity of the ferromagnetic magnetization the triplet superconducting correlations (TSC) may arise in a vicinity of the interface of singlet superconductors [1, 2]. A distinctive feature of the TSC is the insensitivity to the exchange magnetic interaction and the penetration into the ferromagnet over long distances that are typical for a normal (non-magnetic) metal. The occurrence of TSC was proved experimentally by the presence of the superconducting current in the structures of two singlet superconductors connected by a ferromagnetic layer with a helical magnetization [3, 4]. TSC in superconducting structures with a composite ferromagnetic interlayer (S /F_L/F_R/ S) was predicted for ballistic transport [5], as well as in the case of diffuse scattering [6-8]. Recently, abnormally large value of the critical current was found in the mesa- structures YBa₂Cu₃O_{7- δ} /SrRuO₃/La_{0.7}Sr_{0.3}MnO₃/Au-Nb. It was attributed to the excitation of the TSC in the superconducting current in the ferromagnetic interlayer [9, 10].

In the oxide interfaces, for example, at the cuprate superconductor and manganite ferromagnet, the interface transparency is determined by the work function and may be sufficiently low [11]. The often utilized ferromagnetic lanthanum manganite doped with strontium La_{0.7}Sr_{0.3}MnO₃ (LSMO) has

⁴ To whom any correspondence should be addressed



100% spin polarization at low temperatures. An occurrence of spin-triplet excitations is possible in this case while the singlet superconducting correlations are strongly suppressed. This paper presents results of experimental studies of superconducting and quasiparticle currents in superconducting hybrid mesa-structures with composite ferromagnetic interlayer $\text{SrRuO}_3/\text{La}_{0.7}\text{Sr}_{0.3}\text{MnO}_3$. From experimental data the characteristic resistance of interfaces and the coherence length in the ferromagnetic interlayer are estimated.

2. Experimental samples and technique

The mesa-structures of two superconductors, the cuprate with a high critical temperature and metal - Nb coupled by composite layer of two ferromagnets were investigated. The cuprate superconductor $\text{YBa}_2\text{Cu}_3\text{O}_{7-\delta}$ (YBCO) was deposited by laser ablation using an excimer laser Kr (wavelength of 248 nm) on (110) NdGaO_3 (NGO) substrate. It followed by in-situ deposition of two layers of ferromagnets: strontium ruthenate SrRuO_3 (SRO) and $\text{La}_{0.7}\text{Sr}_{0.3}\text{MnO}_3$ (LSMO). YBCO layer with a typical thickness of 80–120 nm is deposited at a substrate temperature of 790° C and oxygen pressure of 0.6 mbar, SRO and LSMO layers were deposited at a substrate temperature of 760° C and oxygen pressure of 0.3 mbar. Further cooling down to 100°C was performed in an oxygen atmosphere with a cooling rate 5–10°C/minute. Then, 20 nm Au film was deposited in-situ at a temperature of 100°C and a pressure of 10^{-5} mbar to prevent the oxidation of the samples in air atmosphere. Next, the Nb layer with 20 nm thickness was deposited by magnetron sputtering ex-situ [9, 10].

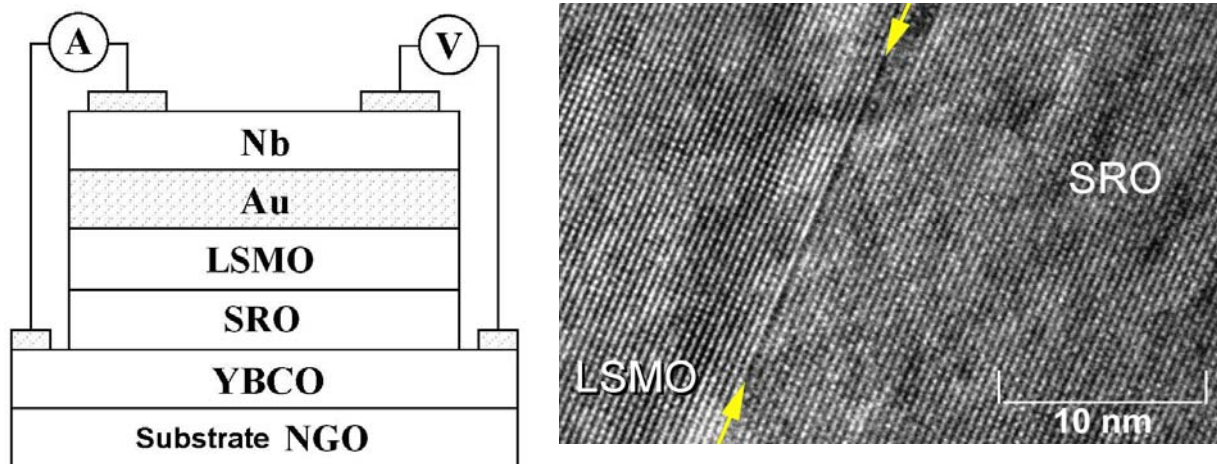


Figure 1. Cross section of mesa-structure and current biasing (left). A is the current source, V is voltmeter. On the right: Transmission Electron Microscope view of SRO/LSMO interface is shown.

The mesa-structures having the linear dimensions in the plane of $L = 10, 20, 30, 40, 50 \mu\text{m}$ were manufactured using photolithography techniques, ion beam etching, and lift-off photolithography. The SiO_2 film with thickness of 40 nm was used for isolation of the sides of the mesa-structure (not shown in Figure 1). The properties of surface of the films were tested by atomic force microscope. The rather sharp boundaries between layers at SRO/LSMO interface were observed by transmission electron microscope (Figure 1). As shown in Figure 1 the SRO/LSMO interface is homogeneous well enough at this scale. More detailed studies of the SRO/LSMO interface by transmission electron microscopy with a correction of aberration showed the presence of mixing of Mn atoms and Ru on a scale of one atomic cell (0.3 nm), as well as of Sr and La on a scale of two atomic cells [12]. Electron energy loss spectroscopy (EELS) showed that an inhomogeneity of oxygen vacancies in the range of 1–2 nm is observed [12, 13].

The cuprate superconductor YBCO film was used as a base electrode providing the epitaxial growth of ferromagnetic oxide layers: LSMO with a coercive force of 2–3 mT and the exchange

energy 2.3 meV [14], and the SRO with the coercive force the order of 1 T and the exchange energy of 13 meV [15].

3. Results and discussion

We investigated more than 25 chips with 5 mesa-structures each one with different linear sizes (L). The layout of the chips remained unchanged but the thicknesses of the ferromagnetic layers were varied. Table 1 summarizes the electrical parameters for some mesa-structures that are discussed in more details.

Table 1. DC parameters of mesa-structures

d_{SRO} and d_{LSMO} are the thicknesses of SRO and LSMO films correspondingly, L and j_C are the linear size of mesa-structure and critical current density, $R_N A$ is characteristic resistance where R_N and $A=L^2$ are normal resistance and the square of mesa-structure, correspondingly.

N	d_{SRO} (nm)	d_{LSMO} (nm)	L (μm)	$R_N A$ ($\mu\Omega \text{ cm}^2$)	j_C (A/ cm^2)
1	8.5	3	10	0.13	25
2	8,5	6	20	0,11	5.7
3	5.6	15	50	0.20	1.1
4	10	9	30	0.15	2.2

3.1. Mesa-structure resistance

The temperature dependence of the mesa-structure resistance $R(T)$ is presented in Figure 2. Above the critical temperature of YBCO (T_C^{YBCO}) $R(T)$ has a linear metallic behavior that is inherent for the temperature dependence of YBCO electrode. At $T \approx T_C^{YBCO}$ the resistance of mesa-structure R is sharply reduced in magnitude. No features that are typical for the temperature dependence of the ferromagnetic films of interlayer [16] were observed. Therefore, below the critical temperature T_C^{YBCO} the contribution of YBCO, LSMO and SRO films resistance can be neglected. The resistance of bilayer film Au-Nb is also small [17]. As a result, at temperatures $T_C^{Nb/Au} < T < T_C^{YBCO}$ the resistance of the mesa-structure consists of the resistance of the following interfaces: YBCO/SRO, SRO/LSMO, LSMO/Au: $R_{MS} = R_{YBCO/SRO} + R_{SRO/LSMO} + R_{LSMO/Au}$.

The characteristic resistance of the mesa-structure $R_N A$ changes from chip to chip from 0.1 to 1 $\mu\Omega \text{ cm}^2$. Most likely this is due to the influence of the LSMO/Au interface, which was subjected to ion cleaning and deposition of Nb ex-situ. However, $R_N A$ less varied over a chip when the size of mesa-structure is changed. To determine the characteristic resistance of barriers the mesa-structures with single ferromagnetic layer were fabricated [16]. $R_N A$ for the mesa-structures with only a SRO layer is almost three orders of magnitude smaller than for the mesa-structure with a LSMO layer. Assuming that the LSMO/Au interface resistance is not greater than 1 $\mu\Omega \text{ cm}^2$ [11, 18] then the resistance of a mesa -structure of YBCO/LSMO/Au can be explained by the resistance YBCO/LSMO interface (100 $\mu\Omega \text{ cm}^2$). Using the data [18] we find that the SRO/Au interface resistance is about 0.05 $\mu\Omega \text{ cm}^2$, and the resistance of YBCO/SRO is less than 0.1 $\mu\Omega \text{ cm}^2$ [11]. The increase of the resistance of the mesa-structures with a composite LSMO/SRO layer compared with resistance of the mesa-structures with the single SRO layer is explained by the contribution from the SRO/LSMO and LSMO/Au interfaces [18]. The data for LSMO/Au interface resistance [11, 18] were obtained for the deposition of a gold layer after cooling of LSMO film (ex-situ), so the resistance of the LSMO/Au interface may be

substantially higher than that the Au film deposited in-situ. Therefore the main contribution to the resistance of the mesa-structure with a composite interlayer most likely is the result of the YBCO/SRO ($0.1\mu\Omega\text{cm}^2$) and LSMO/Au ($0.2\mu\Omega\text{cm}^2$) interfaces.

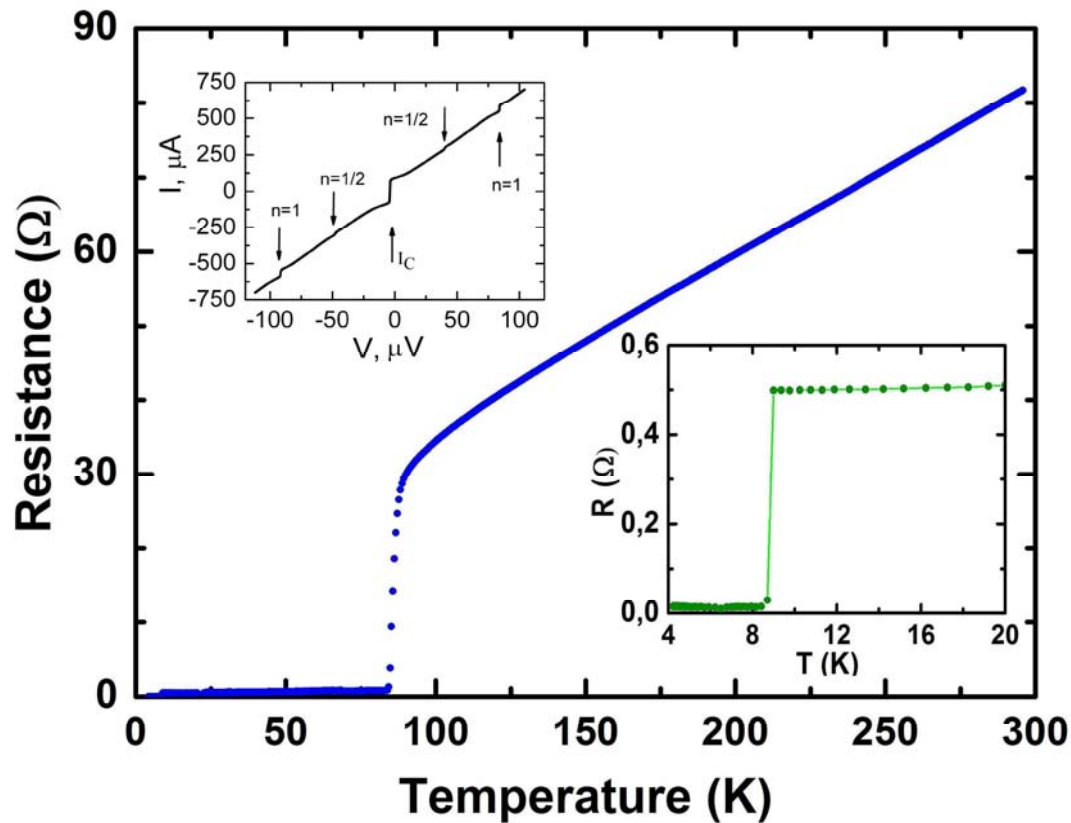


Figure 2. The temperature dependence of mesa-structure resistance N2 $R(T)$, $T_C^{\text{YBCO}}=85\text{ K}$. The part of $R(T)$ for low temperature is shown in right inset, $T_C^{\text{Nb/Au}}=8.7\text{ K}$. The I - V curve of mesa-structure under microwave radiation is shown on the left. The principal and fractional Shapiro steps are shown by $n=1$ and $n=1/2$, correspondingly.

As a result, from $R_N A$ data of mesa-structures we can estimate the average (in the direction of the quasiparticle momentum) transparency of LSMO/Au interface [17]:

$$D = \frac{2\pi^2 \hbar^3}{e^2 p_F^2} \frac{1}{R_N A} = \frac{2\rho^{\text{LSMO}} l^{\text{LSMO}}}{3R_N A}, \quad (1)$$

here p_F is the smallest value of the Fermi momentum of the LSMO and Au. For the following parameters $\rho^{\text{LSMO}} l^{\text{LSMO}} \approx 2 \cdot 10^{-11} \Omega \cdot \text{cm}^2$ and $R_N A = 0.2 \mu\Omega \text{ cm}^2$ the interface transparency is sufficiently small $D \approx 10^{-3}$.

3.2. Critical current

The superconducting critical current was observed at the most mesa-structures with total thickness of the composite layer less than 50 nm. The superconducting current is absent for the mesa-structures with a ferromagnetic (LSMO or SRO) interlayer with the thickness larger than 5 nm. The superconducting current for some samples with thinner interlayer is caused by the current flow

through the pinholes. Existence of the superconducting current for mesa-structures with large thicknesses (>10 nm) of the composite ferromagnetic interlayer [8] is an indication of spin-triplet superconducting correlations presence in it. Contours of critical current densities for experimental thickness variation of magnetic SRO and LSMO layers are shown in Figure 3. The data in figure demonstrate a maximum of critical current density at layer thicknesses $d_{LSMO}=6$ nm and $d_{SRO}=8$ nm. Theoretically, the maximum critical current of mesa-structures with composite interlayer is predicted for thicknesses of ferromagnets of order of the coherence length [7, 19].

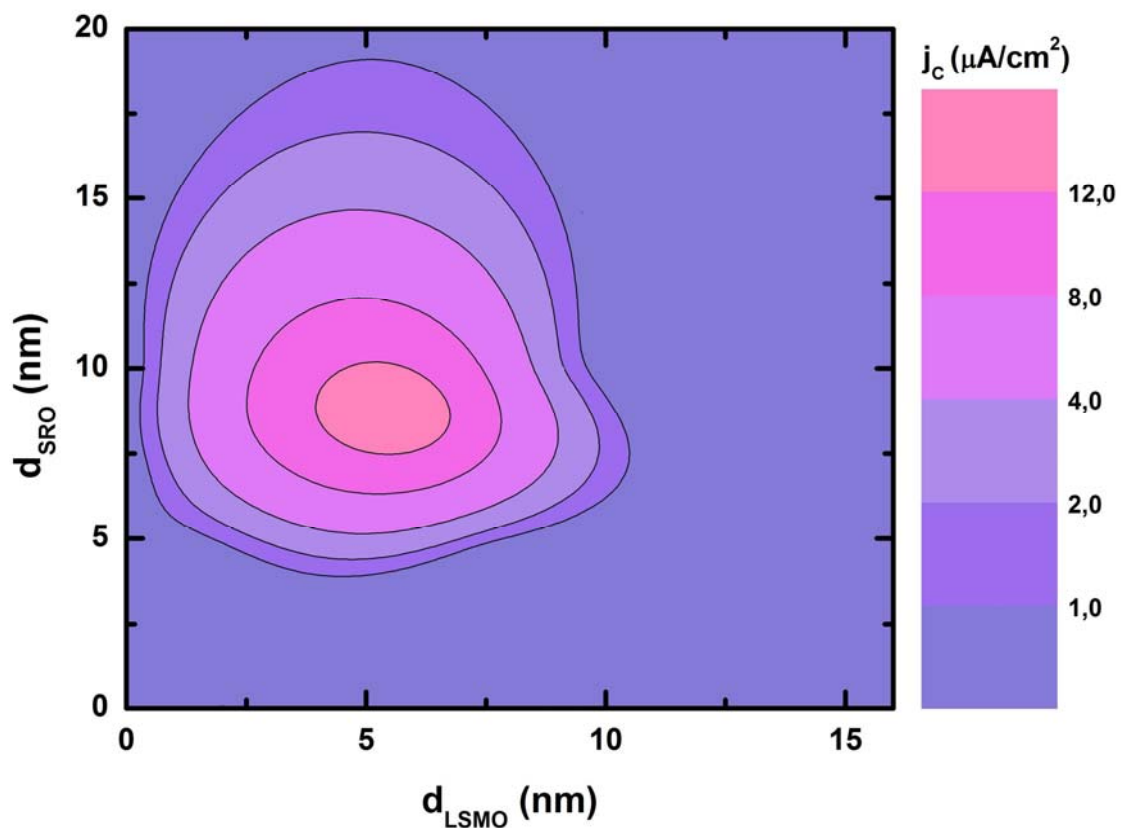


Figure 3. Contours of critical current density vs. the thickness of ferromagnetic layers at $T=4.2$ K. Almost 30 mesa-structures with different thicknesses of interlayer films were used for developing the figure. For mesa-structure with equal d_{LSMO} and d_{SRO} but different j_c the averaged values of critical current density were used.

We estimate the coherence length for ferromagnetic films. Since the mean free path in the oxide materials (SRO and LSMO) is small enough [14, 15], we can assume that the electron transport is diffusive. For the diffusive case the coherence length for the normal material $\xi_N = \left(\frac{\hbar D}{T}\right)^{1/2}$ and for

the ferromagnetic $\xi_F = \left(\frac{\hbar D}{E_{ex}}\right)^{1/2}$, where $D = \frac{1}{3}v_F l$ is the diffusion coefficient and E_{ex} is the

exchange energy. For the used interlayer materials we got for $\xi_F^{LSMO} \approx 8$ nm and $\xi_F^{SRO} \approx 3$ nm. Figure 3 shows that the maximum critical current for the LSMO layer is observed at d_{LSMO} somewhat smaller and for the SRO layer larger than the estimated coherence length. Taking into account the

approximated nature of the coherence length estimation such correspondence to the theoretical prediction should be considered satisfactorily.

4. Conclusion

It is experimentally shown that the thickness dependence of the critical current for a mesa-structure with composite magnetic interlayer varied nonmonotonically with the thickness of both the manganite and ruthenate interlayers. The critical current was observed for total thickness of interlayer up to 50 nm. The maximum value of the critical current density is observed when the thickness of the interlayer is close to the coherence length. The dominance of spin-triplet superconducting correlations in the superconducting current is assumed despite the low transparency of the superconductor-ferromagnetic interface.

Acknowledgments

The partial support by Russian Academy of Science, Scientific School Grant SH-4871.2014.2, Russian Foundation of Basic research № 14-07-00258a, 14-07-93105/14 and Visby project of Swedish Institute. Author also acknowledge to I.V. Borisenko, A.M. Petrzhik, V.V. Demidov for fruitful discussion.

5. References

- [1] Bergeret F S, Volkov A F and Efetov K B 2001 *Phys. Rev. Lett.* **86** 4096
- [2] Kadigrobov A, Shekhter R I and Jonson M 2001 *Europhys. Lett.* **54** 394
- [3] Robinson J W A, Witt J D S and Blamire M G 2010 *Science* **329** 59
- [4] Wang J, Singh M, Tian M, Kumar N, Liu B, Shi C, Jain J K, Samarth N, Mallouk T E and Chan M H W 2010 *Nat. Phys.* **6** 389
- [5] Trifunovic L, Popović Z, and Radović Z 2011 *Phys. Rev. B* **84** 064511
- [6] Crouzy B, Tollis S and Ivanov D A 2007 *Phys. Rev. B* **75**, 054503
- [7] Sperstad B, Linder J and Sudbo A 2008 *Phys. Rev. B* **78**, 104509
- [8] Richard C, Houzet M and Meyer J S 2013 *Phys. Rev. Lett.* **110**, 217004
- [9] Ovsyannikov G A, Sheyerman A E, Shadrin A V, Kislinsky Y V, Constantinian K Y and Kalabuhov A 2013 *JETP Letters* **97**, 145
- [10] Khaydukov Yu N, Ovsyannikov G A, Sheyerman A E, Constantinian K Y, Mustafa L, Keller T, Uribe-Laverde M A, Kislinskii Yu V, Shadrin A V, Kalabukhov A, Keimer B and Winkler D 2014 *Phys. Rev. B* **90** 035130
- [11] van Zalk M, Brinkman A, Aarts J and Hilgenkamp H 2010 *Phys. Rev. B* **82** 134513
- [12] Borisevich A Y, Lupini A R, He J, Eliseev E A, Morozovska A N, Svechnikov G S, Yu P, Chu Y.-H, Ramesh R, Pantelides S. T, Kalinin S V, and Pennycook S J 2012 *Phys. Rev. B* **86**, 140102(R)
- [13] Ziese M, Vrejoiu I, Pippel E, Esquinazi P, Hesse D, Etz C, Henk J, Ernst A., Maznichenko I V, Hergert W and Mertig I 2010 *Phys. Rev. Lett.* **104** 167203
- [14] Woodfield B F, Wilson M L and Byers J M 1997 *Phys. Rev. Lett.* **78** 3201
- [15] Asulin I, Yuli O, Koren G et al. 2009 *Phys. Rev. B* **79** 174524
- [16] Petrzhik A M, Ovsyannikov G A, Shadrin A V, Constantinian K Y, Zaitsev A V, Demidov V V and Kislinski Yu V 2011 *JETP* **112** 1042
- [17] Komissinskiy P, Ovsyannikov G A, Constantinian K Y, Kislinski Y V, Borisenko I V, Soloviev I I, Kornev V K, Goldobin E, and Winkler D 2008 *Phys. Rev. B* **78** 02450
- [18] Mieville L, Worledge D, Geballe T H, Contreras R and Char K 1998 *Appl. Phys. Lett.* **73** 1736
- [19] Volkov A F and Efetov K B 2010 *Phys. Rev. B* **81**, 144522